Int. J. Heat Mass Transfer. Vol. 22, pp. 171–173

0017-9310/79/0101-0171 $02.00/0

PHOTOGRAPHIC STUDY OF MELTING ABOUT AN EMBEDDED HORIZONTAL HEATING CYLINDER

R. M. ABDEL-WAHED, J. W. RAMSEY and E. M. SPARROW
Department of Mechanical Engineering, University of Minnesota, Minneapolis, Minnesota, U.S.A.

(*Received* 15 *March* 1978 *and in revised form* 22 *May* 1978)

INTRODUCTION

THE OBJECTIVE of this note is to provide direct visual information to supplement and extend the results of [1] relevant to the role of natural convection in the melting of solids. In [1], experiments were described in which a horizontal heating cylinder was embedded in a solid at its fusion temperature. By energizing the heater with a constant power input, a steadily growing melt region surrounding the cylinder was created. The heating cylinder was instrumented to provide information about the surface heat-transfer coefficient, and a grid of 92 thermocouples was deployed throughout the phase change medium to detect the passage of the solid–liquid interface. The experiments were performed with a eutectic mixture of sodium hydroxide and sodium nitrate [fusion temperature ~244°C (471°F)].

The experiments demonstrated that natural convection was the dominant mode of heat transfer. One of the evidences of this dominance was the shapes of the melt region. These shapes were inferred from temperature measurements in the phase change medium. Owing to mechanical constraints, it was not possible to make detailed temperature measurements below and at the sides of the cylinder, so that the shapes presented in [1] were confined to the region above the cylinder.

In the present investigation, photographic evidence of actual melt layer shapes was obtained to corroborate those inferred in [1]. The photographs show the melt layer both below and above the cylinder, thereby extending the results of [1]. Another extension was made in connection with the initial state of the solid at the onset of melting. Whereas in [1] all of the experiments were concerned with a solid at its fusion temperature, the present experiments encompassed both that condition and an initially subcooled condition (i.e. initial temperature of the solid lower than the fusion temperature).

The general approach used in the investigation was to embed a horizontal heating cylinder in a solid phase-change material and to create a growing melt region about the cylinder by a steady input of heat. At a preselected time, the heating was discontinued and the liquid was extracted from the melt region by means of suction and gravity. The unmelted solid was allowed to cool to room temperature and then was removed from the test apparatus and cut along a vertical plane, thereby revealing the cross section of the melt cavity. To obtain a clear photographic record of the shape of the cavity, it was filled with a dark sand.

The experiments were performed using the same eutectic salt as in [1].

THE EXPERIMENTS

Although the present apparatus is an entity fully distinct from that of [1], there are similarities in design and fabrication such that only an abbreviated description stressing its essential features need be given here. The heart of the apparatus was a test chamber consisting of a nearly cubical mild steel tank, approximately 33 cm on a side, which housed the phase change material. The test chamber was equipped with a horizontal electrically heated cylinder, 1.9 cm (3/4 in) in diameter and 30.5 cm (12 in) long, situated parallel to a pair of side walls and midway between them. The centerline of the cylinder was positioned about 6 cm (2 3/8 in) above the floor of the tank.

In addition to the heating cylinder, the test chamber was equipped with auxiliary heaters and a cooling coil. These devices were used to avoid the formation of internal cavities during the freezing process which preceded each melting run and to provide a vent for the excess volume of liquid created when melting occurred adjacent to the heating cylinder. The test chamber was encased in insulation, external to which were heating panels which, in turn, were backed by another layer of insulation. The heating panels were used to bring the temperature of the phase change material to the desired level and then to maintain it at that level.

Special features were incorporated into the apparatus to facilitate the extraction of the liquid from the melt cavity. A valve-equipped, heated pipeline was used to connect the test chamber to an auxiliary tank whose function was to receive the extracted liquid melt. The pipeline was positioned so that its centerline was about 1.25 cm (1/2 in) below the centerline of the heating cylinder in the test chamber. Heating of the pipeline was necessary to avoid extraneous heat losses from the test chamber (via the fin effect) and to ensure that the extracted liquid did not freeze en route from the test chamber to the receiving tank.

The receiving tank was designed and fabricated to serve as a vacuum chamber and thereby, via suction, to aid in the extraction of the liquid melt from the test chamber. To this end, the receiving tank was connected to a mechanical vacuum pump.

In practice, drainage by gravity was found to be a more effective extraction mechanism than suction. To facilitate the use of gravity drainage, the entire apparatus (test chamber, pipeline, and receiving tank) was positioned on a rigid base plate which was hinged at one end. Under normal conditions, the base plate was horizontal (in contact with the floor of the laboratory). For the liquid extraction operation, the end of the base plate opposite the hinged end was raised by means of a hoist, at an angle of about 15° to the horizontal. The raising of the base plate caused the liquid to flow from the test chamber into the interconnecting pipeline and then into the receiving tank.

Another feature of the apparatus was the provisions for removing the unmelted solid from the test chamber at the conclusion of a run. In this connection, the side walls of the test chamber were slightly sloped so that the horizontal cross section of the chamber enlarged with height. Owing to the sloping walls and to the fact that the solid contracts as it cools, a gap was established between the unmelted solid and the chamber walls as the apparatus cooled to room temperature after a run. The non-adherence of the solid to the side walls greatly simplified the removal operations. The actual removal was accomplished with the aid of a metal sling whose bottom portion lay on the floor of the test chamber (the sling had been placed in the test chamber when the salt was in its molten form). The sling was raised by a jack-like device that was supported on the side walls of the test chamber.

The solid, as removed, was a rectangular block, approximately $30 \times 30 \times 20$ cm ($12 \times 12 \times 8$ in) in size. It was cut along a vertical plane with a band saw in order to expose the cross section of the melt cavity.

Each data run involved four distinct stages. The first was the melting of the solid to produce a homogeneous liquid having the eutectic composition, and this was followed by the freezing of the liquid to yield a uniform solid, free of internal shrinkage cavities. In the third stage, the external heating panels were employed to bring the solid to the desired initial temperature for the melting experiment —either the fusion temperature or some selected degree of subcooling. The heating of the solid was performed slowly in order to avoid excessive melting adjacent to the walls of the test chamber. During the heating period, the temperature of the solid in the neighborhood of the heating cylinder was monitored with a thermocouple attached to the surface of the cylinder. The last of the four stages was the melting experiment itself, involving the creation of the melt region and the extraction of the liquid.

Under favorable conditions, the four stages of a data run could be accomplished in three to four weeks. The majority of this time was devoted to the heating of the solid to bring it to a uniform initial temperature prior to the melting experiment.

Since the focus of the present study was the visual determination of the melt shapes, the heating cylinder was not instrumented with a sufficient number of thermocouples to enable the evaluation of heat-transfer coefficients.

RESULTS AND DISCUSSION

Photographic results for three experiments will be presented here. The first two of these are for the case in which the solid was at its fusion temperature at the onset of melting, whereas the third is for a case where the solid was subcooled. For all three experiments, the power input to the horizontal heating cylinder was approximately 5700 W/m^2, which corresponds closely to one of the power levels of [1].

The results for the runs with the solid at the fusion temperature are presented in Fig. 1. The photograph at the left corresponds to an elapsed time of 15 min after the onset of heating, whereas the photo at the right is for a heating period of 90 min. In each photograph, the black region represents the melt zone, while the white circle is the horizontal heating cylinder (which, for the photographs, was simulated by a white-painted rod whose diameter is equal to that of the heating cylinder). The white region surrounding the melt zone is unmelted solid. A horizontal line has been drawn in each photograph to depict the location of the floor of the test chamber. The slight irregularities of the solid–liquid interface in evidence in the photographs are due primarily to unavoidable chipping that occurred at the melt cavity surface during the cutting operation.

Aside from the expected result that the melt region grows with time, Fig. 1 provides insights into the transfer processes. At relatively short times (left-hand photo), the extent of the melting above the cylinder is only slightly greater than that below the cylinder. On the other hand, at larger times, the melt region is situated primarily above the cylinder, with relatively little melting below. Thus, while a considerable amount of melting occurred above the cylinder between the 15 min and 90 min observations, the melt region below the cylinder was relatively unchanged during that time interval.

If conduction were the sole heat-transfer mechanism, then, at any instant of time, the melt region would be a concentric annulus surrounding the heating tube. Thus, from Fig. 1, it can be surmised that conduction does play an important role at small times. On the other hand, the resounding departure from the concentric annular configuration at larger times indicates that it is natural convection, rather than conduction, that is dominant. The primary factor in the upward thrust of the melt region is the plume which rises from the top of the heating cylinder. The plume delivers hot liquid to the upper part of the melt region and, in this way, causes further melting to occur there.

The foregoing interpretation of the transfer mechanisms based on Fig. 1 confirms that set forth in [1] on the basis of less complete melt layer shapes. Figure 1 also confirms the assertation of [1] that the floor of the test chamber was sufficiently far removed from the heated cylinder so as not to influence the melting process.

The effect of initial subcooling of the solid on the melting process is shown in Fig. 2. This photograph corresponds to the same heating rate as for Fig. 1 (5700 W/m^2), to the same elapsed heating time as the right-hand photo of Fig. 1 (90 min), but to a subcooling of the solid of about 42°C (75°F). The melt region for the subcooled case is substantially smaller than that without subcooling, as is expected because a portion of the energy input is absorbed as sensible heat by the solid. Also of interest is the shape of the melt region, which is narrower than that for no subcooling. This narrowing can be attributed to the rapid cooling of the liquid plume as it impinges at the top of the melt cavity, making it a less effective melting medium as it recirculates around the sides of the cavity.

Photographs of melting about a horizontal cylinder embedded in a low-temperature phase change material, a paraffin with a 44°C melting temperature, are reported in

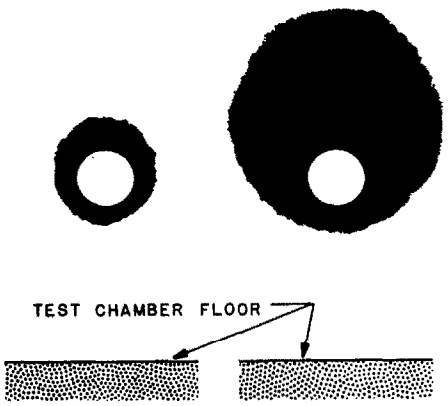

FIG. 1. Melt region shapes in a solid at its fusion temperature. Left: heating period = 15 min; right: heating period = 90 min. Heating power = 5700 W/m^2.

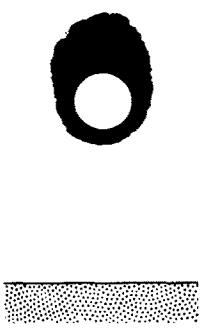

FIG. 2. Effect of subcooling on melting. Extent of subcooling = 42°C (75°F); heating period = 90 min; heating power = 5700 W/m^2.

[2]. The experiments were performed with the solid paraffin at room temperature, which corresponds to a subcooled condition. The results of [2] also indicate that conduction is important only at early times and that natural convection becomes dominant at later times.

Acknowledgement—This research was performed under ERDA grant E(11-1)-2595.

REFERENCES

1. E. M. Sparrow, R. R. Schmidt and J. W. Ramsey, Experiments on the role of natural convection in the melting of solids, *J. Heat Transfer* **100**, 11–16 (1978).
2. R. D. White, A. G. Bathelt, W. Leidenfrost and R. Viskanta, Study of heat transfer and melting front from a cylinder imbedded in a phase change material, ASME paper No. 77-HT-42 (1977).

Int. J. Heat Mass Transfer. Vol. 22, pp. 173–175

0017-9310/79/0101-0173 $02.00/0

LATTICE THERMAL CONDUCTIVITIES OF TiO—MeO (Me=Ni, Co, Mn) SOLID SOLUTIONS

A. KH. MURANEVICH
Department of Inorganic and Analytical Chemistry, The Hebrew University of Jerusalem, Jerusalem, Israel

(*Received* 10 *April* 1978)

NOMENCLATURE

- k_l, lattice thermal conductivity;
- k_0, thermal conductivity of perfect lattice;
- ω_D, maximum frequency of Debye spectrum;
- ω_0, frequency at which probabilities of umklapp scattering and imperfection scattering are equal;
- Γ, scattering parameter;
- V, average volume per atom;
- N, number of molecules per unit volume;
- θ_D, Debye temperature;
- M_i, mass of molecule;
- $\bar{M}$, average mass of molecules of crystal;
- x_i, concentration of molecules of mass M_i;
- k_l^{I}, lattice thermal conductivity calculated for imperfection scattering of phonons by local mass changes;
- k_l^{II}, lattice thermal conductivity calculated for imperfection scattering of phonons by local mass and force-constant changes;
- g, bond constant of nearest metal and oxygen atoms in host lattice;
- g_i, bond constant of impurity atom and its nearest neighbors;
- Δg_i, $(g-g_i)$ difference;
- γ, Gruneisen parameter;
- δ, interatomic distance in host lattice;
- δ_i, impurity radius;
- $\Delta\delta_i$, $(\delta-\delta_i)$ difference;
- α, regulated parameter in Parrott's theory;
- B_N and B_U, scattering factors for N-processes and U-processes.

I. INTRODUCTION

TITANIUM monoxide $TiO_{1\pm x}$ and the iron group metal monoxides $Me_{1-x}O$ (Me=Ni, Co, Mn) have the same crystalline structure (rock salt), but differ considerably in the nature of the interatomic interactions and by the degree of localization of 3d electrons. Accordingly, different TiO—MeO (Me=Ni, Co, Mn) solid solutions formed during the isomorphous substitution of atoms in the metal sublattice have different transport properties, and, in particular, different thermal conductivities.

As reported earlier [1], TiO—MeO (Me=Ni, Co, Mn) solid solutions with a small content of iron group metal atoms have a low lattice thermal conductivity. The electronic and lattice thermal conductivities of these compounds at room temperature are comparable; this is typical of alloys and semimetals containing many imperfections. At high temperatures heat transfer is carried out essentially by free 3d electrons. A similar increase in the electronic contribution to the thermal conductivity with that of temperature was observed in the transition metal carbides and nitrides with high residual electrical resistivities; Williams [2] has explained this effect by the strong scattering of electrons by lattice vacancies. When the concentration of the iron group metal atoms in TiO—MeO (Me=Ni, Co, Mn) solid solutions is increased, the localization of 3d electrons strengthens, so that in solid solutions with a small titanium content the heat is transferred solely by lattice vibrations.

In this paper an analysis of the lattice thermal conductivity data is presented for TiO—MeO (Me=Ni, Co, Mn) solid solutions of different compositions and the phonon scattering processes are considered.

II. EXPERIMENTAL

The experimental details of this study have been described elsewhere [1]. The solid solutions were prepared by the solid-phase reaction method. The composition of the samples and the X-ray and pycnometric data are given in Table 1. The absolute stationary method was used for the thermal-conductivity measurements. The electrical conductivity was measured by the two-probe D.C. potentiometric method.

The lattice thermal conductivities k_l of TiO—MeO (Me=Ni, Co, Mn) solid solutions at room temperature are shown in Fig. 1 and Tables 2 and 3 (for metallic type samples k_l was defined by subtracting the electronic component from the measured total thermal conductivity). A comparison of the above data with the theory of heat transfer in solid solutions is presented below.

III. DISCUSSION OF RESULTS

According to Klemens [3], the thermal conductivity of solid solutions in the case of strong imperfection scattering can be expressed as

$$k_l = k_0 \frac{\omega_0}{\omega_D} \tan^{-1}\left(\frac{\omega_D}{\omega_0}\right) \quad (1)$$

where k_0 is the thermal conductivity of a perfect crystal lattice, ω_D, the maximum frequency of the Debye vibration spectrum and ω_0, the frequency at which the probabilities